# A refined human linear B cell epitope map of Outer surface protein C (OspC) from the Lyme disease spirochete, *Borreliella burgdorferi*

Grace Freeman-Gallant[1,#], Kathleen McCarthy[2, #], Jennifer Yates[1,2], Karen Kulas[1], Michael J. Rudolph[3], David J Vance[1,2], and Nicholas J Mantis[1,2,*]

[1] Division of Infectious Diseases, Wadsworth Center, New York State Department of Health, Albany, NY; [2] Department of Biomedical Sciences, University at Albany, Albany, NY;[3] New York Structural Biology Center, New York, NY

[#], these authors contributed equally to this study with last names listed alphabetically

**Running title:** Linear B cell epitopes on OspC

*, address correspondence to Dr. Nicholas Mantis, Division of Infectious Diseases, Wadsworth Center, New York State Dept Health, 120 New Scotland Ave, Albany, NY 12208; Tel: 518-473-7487; Email:nicholas.mantis@health.ny.gov

**ABSTRACT**

A detailed understanding of the human antibody response to Outer surface protein C (OspC) of *Borrelellia burgdorferi* has important implications for Lyme disease diagnostics and vaccines. In this report, a total of 13 peptides encompassing eight reported OspC linear B cell epitopes from OspC types A, B and K, including the conserved C-terminus (residues 193-210: peptide C10), were evaluated by multiplex immunoassay (MIA) for IgG reactivity with ~700 human serum samples confirmed positive in a two-tiered Lyme disease diagnostic assay and ~160 post-treatment Lyme disease (PTLD) serum samples. The VlsE C6-17 peptide was included as a positive control. Diagnostic serum IgG reacted with 11 of the 13 OspC-derived peptides, significantly more than controls, with the C10 peptide being the most reactive. In the PTLD serum samples, two OspC peptides including C10 were significantly more reactive than controls. Spearman's rank correlation matrices and hierarchical clustering indicated a strong correlation between C10 and VlsE C6-17 peptide reactivity but little demonstrable association between C10 and the other OspC peptides or recombinant OspC. OspC peptide reactivities (excluding C10) were strongly correlated with each other and were disproportionately influenced by a subset of pan-reactive samples. In the PTLD cohort, C10 clustered with the other OspC-derived peptides and was distinct from OspC and VlsE C6-17. The asynchronous serologic response to OspC, C10, and the OspC-derived peptides reveals the complexity of B cell responses to *B. burgdorferi* and confounds simple interpretation of antibody profiles associated with Lyme disease.

**IMPORTANCE**

Lyme disease is an emerging tick-borne infection caused by the spirochete, *Borreliella burgdorferi*. In humans, antibodies against spirochetal outer surface lipoproteins are proposed to play a role in disease resolution and in protection against reinfection. Some of those same antibodies also serve as diagnostic indicators of an active or history of Lyme disease. In this study, we sought to validate reported antibody binding sites on Outer surface protein C (OspC), a known target of both protective and diagnostic antibodies.

**KEYWORDS:** Lyme disease, antibody, epitope, vaccine, *Borrelia burgdorferi*

56 **INTRODUCTION**

57 Lyme (borreliosis) disease is the most common vector-borne infection in the United
58 States, with an estimated 450,000 cases per year (1). The primary etiologic agent of Lyme
59 disease is the spirochetal bacterium, *Borreliella burgdorferi*. In North America, the spirochete is
60 transmitted to humans by black legged ticks, *Ixodes scapularis* and *Ixodes pacificus*, during the
61 course of a blood meal. The spirochete proliferates at the site of the tick bite, typically resulting
62 in an expanding skin lesion commonly referred to as erythema migrans (2-4). In the absence of
63 antibiotic intervention, *B. burgdorferi* can disseminate to peripheral tissues, organs, joints, and
64 the central nervous system, potentially resulting in complications including neuroborreliosis,
65 carditis and/or Lyme arthritis weeks, months or even years later (2, 5). Moreover, a small
66 fraction of Lyme disease patients who receive a full regimen of antibiotics will report persistent
67 health issues (e.g., fatigue, cognitive issues, musculoskeletal pain), a difficult to define syndrome
68 termed post-treatment Lyme disease (PTLD) (6-9). Developing rapid and accurate diagnostic
69 tests capable of detecting and discriminating between LD, PTLD syndrome and *B. burgdorferi*
70 reinfection are much needed (2l, 10).

71 The humoral response to *B. burgdorferi* is robust, resulting in detectable spirochete-
72 specific B cells and serum IgM and IgG days and weeks following an infectious tick bite (11-
73 14). In Lyme disease patients, antibodies are primarily directed against *B. burgdorferi*'s panoply
74 of outer surface lipoproteins (15). Among these, Outer surface protein C (OspC; also known as
75 BB_B19, P23 and P25) stands out. OspC is a ~21 kDa helical homodimeric lipoprotein
76 expressed by *B. burgdorferi* during tick transmission and in the early stages of infection (16).
77 OspC is implicated in facilitating spirochete egress from the tick during the course of a blood
78 meal, enabling survival in the early stages of mammalian skin infection, and modulating
79 transmigration across vascular walls (16-23). The highly immunogenic nature of OspC has lent
80 itself to applications in Lyme disease serology-based diagnostics, including widely used
81 commercial tests (24, 25). For example, the peptide derived from the conserved C-terminal 10
82 amino acids of OspC (peptide "C10") is a component of the FDA approved diagnostic test
83 *Borrelia* VlsE1/pepC10 from Zeus Scientific (Branchburg, NJ) (26-30). In addition to their
84 diagnostic utility, linear B cell epitopes from different OspC types are a component of a widely
85 used canine Lyme disease vaccine and being considered for human use (see references within
86 (31)).

87 While multiple linear human B cell epitopes on OspC have been reported over the past
88 three decades, differences in serologic assays, detection methodologies, and sample sizes from
89 varying Lyme disease cohorts, makes it difficult to draw conclusions about relative reactivities of
90 one peptide over another. This is problematic, because determining the relationships between
91 OspC-derived peptides (including C10) and total OspC antibodies has practical implications for
92 interpreting serologic assays. Moreover, there are >26 allelic variants or types of OspC reported
93 in the United States, with amino acid sequence identities that range from 60-90% (32, 33). As
94 different OspC types are associated with varying degrees of virulence and invasiveness, tracking
95 epitope-specific responses to those particular types is of paramount importance (34, 35). In New
96 York state, for example, OspC types A, B and K, which are associated with more invasive
97 disease, represent ~70% of all isolates (35-37).
98 With that in mind, we sought to validate human antibody reactivities to reported linear epitopes
99 associated with OspC types A, B, and K to enable broad comparability of epitope usage across
100 *B. burgdorferi* for diagnostic and vaccine development purposes.
101
102 **METHODS**
103
104 **Chemicals and biological reagents**. Chemicals and reagents were obtained from Thermo Fisher
105 Scientific (Waltham, MA), unless noted otherwise. Buffers were prepared by the Wadsworth
106 Center's Cell and Tissue Culture core facility.
107
108 **Recombinant OspC and OspC-derived peptides.** Recombinant *B. burgdorferi* $OspC_A$
109 (residues 38 to 201; PDB ID 1GGQ; UniProt ID Q07337) (38), $OspC_B$ (residues 38 to 202; *B.*
110 *burgdorferi* strain ZS7; PDB ID 7UJ2) (39) and $OspC_K$ (residues 38 to 202; *B. burgdorferi* strain
111 297; PDB ID 7UJ6) (40) were expressed in *E. coli* strain BL21 (DE3) and purified by nickel-
112 affinity and size-exclusion chromatography, as described (41). Recombinant $OspC_A$ with the C10
113 sequence (residues 201-210; PVVAESPKKP; "$OspC_A$+C10") was expressed and purified as
114 above. Linear epitope prediction was done using Discotope 2.0 (42). OspC peptides (>80%
115 purity) as described in **Table 1** were synthesized by Genemed Synthesis (San Antonio, TX) with
116 a C-terminal GGGSK-biotin extension. We also synthesized the VlsE-derived C6 B31-17 peptide
117 [MKKDDQIAAAIALRGMA] with the GGGSK-biotin linker (43).

118

119 **Commercial and clinical LD serum samples.** Commercial Lyme disease seronegative (Lot
120 10500586) and seropositive (Lot 10510438) pooled samples were used strictly as intra-assay and
121 bead coupling confirmation controls throughout this study (ACCURUN products 810 and 130,
122 respectively; SeraCare, Milford, MA). The Lyme disease seronegative samples (referred to as
123 "controls" throughout the manuscript) consist of a commercial panel of 81 serum samples
124 collected in 2017-2018 (Access Biologicals, Vista, CA). Five of the 81 serum samples were
125 classified as extreme outliers for VlsE C6-17 reactivity by interquartile range (IQR) calculated
126 using Microsoft Excel and therefore removed from the control panel. In the end, a total of 76
127 control samples were used as comparators with the diagnostic sample set and 75 samples were
128 used as comparators for the PTLD sample set as a result of sample availability.
129 *B. burgdorferi* seropositive serum samples (n = 696) were obtained from the New York
130 State Department of Health Wadsworth Center's Diagnostic Immunology Laboratory. The
131 samples had been submitted for Lyme disease serology and subjected to two-tiered testing
132 consisting of (Tier 1) a C6 peptide screen (Immunetics®; C6 Lyme ELISA™) or Enzyme
133 Linked Fluorescent Assay (ELFA; BioMerieux, VIDAS® Lyme IgG II and Lyme IgM II;
134 Durham, NC), followed by (Tier 2) IgM and IgG detection by Western blot (MarDX®; Trinity
135 Biotech, Carlsbad, CA). *B. burgdorferi*-specific IgM reactivity was defined as ≥2 positive bands,
136 with IgG reactivity defined as ≥5 positive bands. Serum samples were aliquoted, de-identified,
137 and classified as IgM-positive/IgG-negative, IgM-positive/IgG-positive, or IgM-negative/IgG-
138 positive, based on the Western blot results. Post-treatment Lyme disease (PTLD) serum samples
139 (n=158) were kindly provided by the Lyme Disease Biobank at Nuvance Health® (Danbury, CT).
140 PTLD was defined as described by Aucott (8).
141

142 **Multiplexed OspC and OspC peptide microsphere immunoassays (MIA).** Recombinant
143 $OspC_A$, $OspC_B$, or $OspC_K$ (5 µg) were coupled to Magplex-C microspheres (1 x $10^6$) using sulfo-
144 NHS (N-hydroxysulfosuccinimide) and EDC [1-ethyl-3-(3-dimethylaminopropyl) carbodiimide
145 hydrochloride], as recommended by the manufacture (Luminex Corp., Austin, TX). Coupled
146 beads were diluted in xMap® AbC Wash Buffer to a concentration of 5 x $10^6$ beads/ml. Biotin-
147 labeled peptides were complexed to Magplex®-avidin microspheres following protocols provided
148 by the manufacturer (Luminex Corp.). Microspheres were resuspended in 250 µL of assay buffer

149 (1 x PBS, 2% BSA, pH 7.4) then subjected to vortexing and sonication. A total of 1 x $10^6$ beads
150 in assay buffer was mixed with biotin-conjugated peptides (~5 µg) and incubated for 30 min at
151 room temperature. The microsphere suspensions were then washed three times using wash buffer
152 (1 x PBS, 2% BSA, 0.02% TWEEN-20, 0.05% Sodium azide, pH 7.4) and a magnetic separator,
153 resuspended in 500 µL of assay buffer, and stored at 4ºC until use. Successful coupling of OspC
154 and peptides to the Magplex-C microspheres was confirmed by reactivity with immune serum
155 and/or monoclonal antibodies.
156 For experimental use, assay buffer was used to dilute bead stocks (1:50) and human
157 serum (1:100). The bead dilution (50 µL) and diluted serum (50 µL) were combined in black,
158 clear-bottomed, non-binding, chimney 96-well plates (Greiner Bio-One, Monroe, North
159 Carolina) and allowed to incubate for 60 min in a tabletop shaker (600 rpm) at room temperature.
160 Plates were washed three times using a magnetic separator and wash buffer. Secondary antibody
161 goat anti-Human IgG Fc, eBioscience (Invitrogen, Carlsbad, CA) was diluted 1:500 in assay
162 buffer and added (100 µL) to each well. The secondary antibody was allowed to incubate for 30
163 min in a tabletop shaker (600 rpm) at room temperature. Plates were washed as stated above and
164 beads were resuspended in 100 µL of wash buffer. Samples were analyzed using a FlexMap 3D
165 (Luminex Corp). We defined reactivity as the mean MFI +6 SD, based on previous studies
166 conducted in the Wadsworth Center's clinical laboratories (44, 45). Index values were calculated
167 using the sample MFI divided by the reactive cutoff for each bead set (*i.e.*, each peptide coated
168 bead versus itself) such that an index values of >1.0 indicates positive reactivity for a given bead
169 set.
170
171 **Statistical analysis.** Statistical analyses were performed using R 4.3.0 with R packages readxl
172 and tidyverse (46-48). MFIs ($log_{10}$) were first subjected to the Shapiro-Wilk's test to assess
173 normality, then either Levene's or Fligner-Killeen tests to compare variances. Mann-Whitney U
174 tests with an alpha level of 0.05 were used to determine statistical significance for reactivity
175 determination of OspC subtypes and OspC-derived peptides. R package corrplot (49) was used to
176 generate the Spearman's Rank correlation matrix. R package pheatmap was used to create the
177 hierarchically clustered heatmaps (50). R packages ggthemes
178 [https://github.com/jrnold/ggthemes], RColorBrewer [https://cran.r-

179 project.org/web/packages/RcolorBrewer/index.html ], and ggpubr [https://CRAN.R-
180 project.org/package=ggpubr] were used in formatting.
181
182 **Molecular modeling.** PyMol (PyMOL Molecular Graphics System, Version 3.0 Schrödinger,
183 LLC) was used for epitope modeling using OspC PDB ID: **1GGQ** (strain B31, $OspC_A$).
184
185 **RESULTS**
186 We sought to validate the reactivity of OspC linear B cell epitopes, including those
187 already accessioned in the Immune Epitope Database (iedb.org), that have been directly or
188 indirectly implicated in Lyme disease diagnostics and/or immunity to *B. burgdorferi*. Eight
189 different epitopes, including the C10 peptide, were chosen for analysis **(Table 1)**. When localized
190 onto the structure of $OspC_A$ using PyMol, the epitopes represent ~30% of the surface area of the
191 molecule (**Figure 1A**). An alignment of the primary amino acid sequences of the three OspC
192 types (A, B, K) associated with invasive disease in northeast United States revealed
193 polymorphisms in a number of these epitopes (**Table 1**; **Figure 1B**) (51, 52). For this reason, a
194 total of 13 different peptides were generated to encompass the specific amino acid sequences for
195 each epitope within $OspC_A$, $OspC_B$, and $OspC_K$ (**Table 1**). The peptides were synthesized with a
196 C-terminal biotin tag and coupled to streptavidin-coated microspheres for multiplex
197 immunoassays (MIA) by Luminex. As a positive control, we also coupled microspheres with the
198 VlsE C6 B31-17 peptide from *B. burgdorferi* strain B31(43).
199 We employed two *B. burgdorferi* seropositive serum sample collections to gauge the
200 relative reactivity of recombinant OspC, OspC-derived peptides, and the VlsE C6-17 peptide. A
201 "diagnostic" collection consisted of 696 de-identified human serum samples from the Wadsworth
202 Center's Diagnostic Immunology laboratory classified as *B. burgdorferi* seropositive and
203 categorized based on Western blot banding profiles, as $IgM^+/IgG^-$ (+/-), $IgM^+/IgG^+$ (+/+), or $IgM^-$
204 $/IgG^+$ (-/+). A second collection provided by the Lyme Disease Biobank at Nuvance Health
205 consisted of 158 serum samples from PTLD patients. These two collections were compared to a
206 commercial panel consisting of ~75 serum samples confirmed negative for VlsE C6-17 peptide
207 reactivity. We examined both serum IgG and IgM (see Supplemental Information) reactivity
208 profiles.

209 We found that the diagnostic immunology samples were significantly more reactive with
210 recombinant OspC than the control samples, although reactivity was skewed towards $OspC_A$ and
211 $OspC_B$ more than $OspC_K$ **(Figure 2A)**. In terms of peptides, the diagnostic serum samples were
212 on average significantly more reactive than control serums samples with all the OspC-derived
213 peptides tested, except for peptides $71\text{-}86_A$ and $178\text{-}187_B$ (**Figure 2A**). The average serum IgG
214 reactivity was highest against $193\text{-}210_A$ ("C10") and VlsE C6-17 ($p<0.0001$) with the remainder
215 of the peptides being low to moderately reactive relative to the control. Analysis of IgM
216 antibodies revealed significant reactivity with OspC types A, B and K but considerably less
217 reactivity with OspC-derive peptides. Significant IgM reactivity in the diagnostics samples
218 relative to controls was only observed for peptides $9\text{-}33_{ABK}$, $155\text{-}169_A$, $178\text{-}187_{B,\,K}$, and 193-
219 $210_A$ ("C10") (**Figure S1**).
220 To apply a more rigorous evaluation of peptide reactivity, MFI values were subjected to a
221 cutoff value of $\geq$6 SD above the mean of the control MFI, $\log_{10}$ transformed, then plotted to
222 reveal both the number of serum samples above the cutoff (% positive) as well as the magnitude
223 of samples over the cutoff (fold increase). We also derived box and whisker plots to illustrate the
224 upper and lower quartiles as well as the median reactivity to each antigen/peptide with
225 superimposed violin plots to outline sample distribution. Using these metrics, reactivity with
226 $OspC_A$, $OspC_B$ and $OspC_K$ ranged from 24-42% of the diagnostic samples with the fold increase
227 ranging from 2.8 to 4.7 (**Table 2**; **Figure 3A**). In terms of peptides, VlsE C6-17 was the most
228 reactive (71% positive; fold increase 5.8), followed by $193\text{-}210_A$ ("C10") (26% positive; fold
229 increase 4.4) (**Table 2; Figure 3B**). The percent of samples >6SD for the other 12 peptides
230 ranged from 0.1 to 10% with the fold increase between 1.2 and 2.5 (**Table 2; Figure 3B**).
231 Lowering the cutoff threshold to >3 SD resulted in higher overall peptide reactivities, as
232 expected, but the pattern remained the same as >6SD (**Table S1**). Thus, within a given cohort of
233 *B. burgdorferi* seropositive samples, serum IgG reactivity to OspC-derived peptides (apart from
234 $193\text{-}210_A$) is limited to a small subset of individuals, which has important consequences for use
235 of such peptide in diagnostic applications. In terms of IgM reactivity, the trends were similar to
236 IgG except that the most pronounced antibody interactions were with peptides $177\text{-}186_{B,\,K}$
237 followed by $155\text{-}169_A$ and $193\text{-}201_A$ (**Table S2**). The differential peptide reactivity profiles
238 between IgG and IgM might have diagnostic utility.

239 The same overall serologic analysis was performed with a panel of PTLD samples. The
240 PTLD samples were significantly more reactive with $OspC_A$, $OspC_B$ and $OspC_K$ than the control
241 serum samples (**Figure 2B**). For $OspC_A$ and $OspC_K$, 16 and 18% of the samples were above the
242 ≥6SD cutoff with the fold increase between 2.8-5 (**Table 2; Figure 3C**). In the case of $OspC_B$,
243 only 3.2% were above the cutoff with a fold increase of 2.1 (**Table 2; Figure 3C**). In terms of
244 linear epitopes, reactivity significantly above controls was limited to VlsE C6-17 (40% positive;
245 fold increase 5.6), 193-$210_A$ ("C10") (14% positive; fold increase 3.3), and 178-$187_K$ (9.5%;
246 positive; fold increase 3.0) (**Table 2**: **Figure 2B**; **Figure 3D**). Comparatively, PTLD samples had
247 significantly less reactivity to peptide 9-$33_{ABK}$ relative to controls (**Figure 2B**). Only a small
248 fraction of the PTLD serum samples were found to be positive for the remaining 10 peptides
249 (range 1.3-9.5%) and the MFIs did not achieve statistical significance (**Table 2; Figure 2B**).
250 PTLD samples were plotted to visualize OspC and peptide reactivities relative to the cutoff
251 (**Figure 3C-D**). There is notably less reactivity to both 193-$210_A$ ("C10") and C6-17 in the
252 PTLD cohort in comparison to the diagnostic population (**Figure 3B, 3D**).
253 Understanding the relationships between OspC and OspC-derived peptide epitopes has
254 implications for Lyme disease diagnostics and possibly immunity to *B. burgdorferi*. We expected
255 that antibody reactivity with the OspC-derived peptides would strongly correlate with overall
256 OspC antibody levels in any given sample, suggesting that the two populations track with each
257 other and serve as redundant indicators of a previous *B. burgdorferi* infection. To investigate
258 these relationships, we generated correlation matrices (Spearman's Rank) showing the
259 correlation between OspC and the each of the different OspC-derived peptides, including C10
260 and C6-17 (**Figure 4**). While all correlations were determined to be positive, in the diagnostic
261 samples, C10 reactivity was only weakly correlated with $OspC_A$, $OspC_B$, or $OspC_K$ [$r_s$ = 0.2-0.4]
262 (**Figure 4A**). Rather, C10 reactivity was moderately to strongly correlated with other OspC-
263 derived peptides, including 132-$146_A$ ($r_s$ = 0.63), 183-$190_{AB}$ ($r_s$ = 0.58), and 40-$55_{ABK}$ ($r_s$ = 0.58).
264 Indeed, inter-peptide correlations were generally strong across the board (e.g., 132-$146_B$ versus
265 177-$186_A$, $r_s$ >0.9). A similar pattern was observed in the PTLD samples: OspC-derived peptide
266 reactivities were strongly correlated with each other ($r_s$ = 0.63-0.98), but weakly correlated with
267 $OspC_A$, $OspC_B$, and $OspC_K$ ($r_s$ = 0.2-0.4) (**Figure 4B**). In the case of VlsE C6-17, reactivity was
268 weakly correlated with OspC and OspC-derived peptides in both the diagnostic and PTLD
269 samples, except for moderate correlativity with 193-$210_A$ ("C10") in the PTLD cohort ($r_s$ =

270 0.56). These results reveal a significant degree of discordance (asynchrony) among circulating
271 antibody levels against OspC, OspC-derived peptides and the VlsE C6-17 peptide in both
272 diagnostic and PTLD cohorts.

273 The absence of a strong correlation between antibody levels to OspC and OspC-derived
274 peptides led us to subject the diagnostic and PTLD datasets to hierarchical clustering (HC) as
275 means to identify possible relationships in immunoreactivity profiles. In the case of the
276 diagnostic samples, the horizontal (top) dendrogram revealed three distinct branches consisting
277 of (1) $OspC_A$, $OspC_B$, and $OspC_K$, (2) C6-17 and $193\text{-}210_A$ ("C10"), and (3) the other OspC-
278 derived peptides (**Figure 5A**). In cluster 1 ($OspC_A$, $OspC_B$, $OspC_K$), high MFI values were
279 distributed throughout the column with a concentration towards the lower quartile. There was no
280 obvious clustering on the vertical dendrogram to indicate a relationship between OspC reactivity
281 and seropositivity categories (i.e., $IgM^{+/-}$, $IgG^{+/-}$).

282 In branch 2, high VlsE C6-17 reactivity was present throughout the column, albeit, with
283 three hot (orange and red shading) zones and one cold (deep blue shading) zone. In the $193\text{-}210_A$
284 ("C10") column, there was generally an even distribution of MFI intensities only occasionally
285 punctuated with hot spots that often mirror $193\text{-}210_A$ ("C10") reactivity. Samples that were
286 "cold" for C6-17 and $193\text{-}210_A$ ("C10") tended to be within the IgM+/IgG- pool, possibly
287 indicative of an early response to *B. burgdorferi* infection.

288 There were several interesting patterns within branch 3, which consisted of OspC-derived
289 peptides: uniformly <u>low reactivity</u> with peptide $9\text{-}33_{ABK}$, as noted in Figures 2 and 3; a
290 subpopulation of samples that were uniformly <u>nonreactive</u> with all the OspC peptides, as
291 evidenced by a blue band across the top of the figure, which in some instances spilled over to
292 $193\text{-}210_A$ ("C10") and VlsE C6-17 columns; and, finally, a subpopulation of samples with
293 <u>moderate to high</u> pan-OspC peptide reactivity, as evidenced by a horizontal band of orange/red
294 shading situated in the lower third of the figure. Collectively, the HC analysis reveals a
295 remarkable degree of discordance in serum antibody profiles associated with *B. burgdorferi*
296 seropositivity within the diagnostic samples.

297 The HC plot of the PTLD serum samples was clearly distinct from the diagnostic samples
298 (**Figure 5B**). On the horizontal dendrogram, for example, there were just two major branches not
299 three: one encompassing $OspC_{ABK}$ and C6-17, and the other containing the OspC-derived
300 peptides, including $193\text{-}210_A$ ("C10"). On the vertical dendrogram, there were two branches: the

301 top branch corresponding to low peptide reactivity with or without concomitant C6-17 and OspC
302 reactivities; and the bottom branch corresponding to high peptide reactivity that were more
303 frequently than not associated with high C6-17 reactivity. Within the bottom branch, there was a
304 notable subbranch corresponding to 4 samples with strikingly high reactivity with C10, C6-17,
305 and most of the OspC-derived peptides (including 9-33$_{ABK}$). We would tentatively classify these
306 handful of samples as "polyreactive" (53).

307 **Contribution of C10 to overall OspC antibody reactivity**. There is some debate as to
308 what proportion C10-specific antibodies constitute relative to total OspC antibodies, with some
309 studies reporting that C10-specific antibodies make up an overwhelming proportion (54), while
310 others suggesting the opposite (55). As our prior analysis included truncated derivatives of OspC
311 that lacked C10, we expressed a second version of OspC in which residues 202-210
312 (VVAESPKKP) were included. We then revisited Luminex analysis in which we compared MFI
313 to OspC$_A$ versus OspC$_A$+C10. MFIs for OspC$_A$+C10 were significantly greater than OspC$_A$ in
314 both diagnostic and PTLD cohorts, demonstrating that antibody reactivity to the conserved C-
315 terminal residues constitute an important component of the overall antibody response ($p < 0.05$;
316 Mann-Whitney U test) (**Figure 6A, 6D**). We then investigated the relationship between C10
317 reactivity and OspC$_A$ vs OspC$_A$+C10 using a linear regression model for diagnostic samples
318 (**Figure 6B, 6C**) and PTLD samples (**Figure 6E, 6F**). There is a slight increase (0.0702) in the
319 adjusted R-squared value between the C10 peptide MFI and OspC$_A$+C10, as compared to OspC$_A$
320 for the DI cohort (**Figure 6B, 6C**). A similar increase (0.0848) in the adjusted R-squared value
321 was observed between the C10 peptide and OspC$_A$+C10 in comparison to OspC$_A$ for the PTLD
322 population. However, the overall adjusted R-squared value was negligible, thereby
323 demonstrating that C10-specific antibodies constitute only a small fraction of the total OspC
324 reactivity.
325

326 **DISCUSSION**

327 Defining the breadth and the frequency of linear B cell epitope reactivity on OspC has
328 important implications for both Lyme disease diagnostics and vaccines. In this report, a panel of
329 peptides representing eight previously reported and predicted linear epitopes on OspC types A, B
330 and K, were examined by multiplex immunoassay for serum IgG reactivity in diagnostic (n~700)
331 and PTLD (n~150) *B. burgdorferi* seropositive sample sets. The results revealed that seven of the

332 eight peptides are indeed antibody targets even though reactivity to any given peptide may be
333 confined to a fraction (2-10%) of the total samples tested. The exception being peptide C10,
334 which was 26% positive (4.4 positive fold increase value) in the diagnostic sample set and 14%
335 positive (3.3 positive fold increase value) in the PLTDs sample set. Interestingly, in the
336 diagnostic sample set, C10 antibody titers did not correlate with either reactivity to OspC itself or
337 any of the other OspC-derived peptides. In the PTLD sample set, C10 antibody levels did
338 correlate with the other OspC-derived peptides but were distinct from OspC. These results have
339 clinical implications, as they demonstrate that the human B cell response to linear epitopes on
340 OspC is both variable and asynchronous.

341 The C10 peptide corresponds to the stretch of ~10 highly conserved amino acids at C-
342 terminus of OspC, first recognized as an immunodominant epitope in neuroborreliosis patients
343 (54). Since then, the C10 peptide and derivatives have been integrated into numerous diagnostic
344 assays, including the Zeus VlseE1/C10 ELISA (25, 27, 28). Dolange and colleagues recently
345 proposed the use of high affinity C10-specific monoclonal antibodies as tools to detect
346 circulating levels of *B. burgdorferi* antigens (56). While there is little debate as to whether C10
347 constitutes a human B cell epitope, the issue of whether antibodies to C10 contribute to
348 borreliacidal activity remains contentious. Lovrich and colleagues reported that OspC-specific
349 borreliacidal activity (in a handful of human serum samples) was almost entirely directed against
350 C10 (57, 58), whereas Izac and colleagues argued that, in rodents, canines and non-human
351 primates, C10-specific antibodies contribute little if any borreliacidal activity (59). Although our
352 results do not resolve this issue per se, they do raise questions about the underlying B cell
353 biology associated with antibodies to C10 and OspC. The fact that C10 and OspC antibody titers
354 did not correlate with each other in the two serum sample sets examined suggests differences in
355 the kinetics of antibody induction, circulating half-life, and/or plasma cell persistence. Others
356 have suggested, at least in the case of VlsE, there is a distinct progression of epitope reactivity
357 over the course of *B. burgdorferi* infection with readily accessible epitopes targeted first and
358 more obstructed, membrane proximal epitopes following (60). Resolving detailed questions
359 about the nature of the human B cell response to OspC is becoming more feasible as single cell
360 $V_H$ and $V_L$ repertoires are catalogued over the course of Lyme disease (11, 61).

361 B cell epitope prediction software like Discotope 3.0 identifies residues 133-147 as
362 having a high immunogenic propensity (62). That prediction was borne out in our study, as

363 evidenced by statistically significant reactivity of serum samples with the three peptides
364 corresponding to residues 132-146$_{AB}$ and 133-147$_{K}$. Others have reported similar findings in
365 mice and in a few human samples. Namely, Earnhart recognized residues 136-150 (which they
366 refer to as "loop 5") as a target of antibodies in *B. burgdorferi*-infected mice (36). In a follow-up
367 study, the same investigators identified two serum samples from early Lyme disease patients that
368 reacted with peptides spanning 136-144 (63). A subsequent report by Arnaboldi and colleagues
369 did not detect binding to three different 15-mer OspC$_{K}$-derived peptides spanning residues 131-
370 155, possibly because their sample size was limited (27). In our collection of almost 700
371 diagnostic samples, the frequency of peptide positivity was admittedly relatively low (3-7%).
372 Nonetheless, antibodies targeting this epitopic region may be consequential in terms of
373 promoting spirochete clearance (36). For example, the potent borreliacidal mouse monoclonal
374 antibody 16.22 recognizes OspC$_{A}$ residues 133-147 with the key contact points postulated to be
375 residues 139-141 ("KXK" motif) (64). Thus, a more detailed examination of B cell epitopes
376 within this region of OspC in human Lyme disease patients is warranted.
377 It has been postulated that serum antibody profiling at the antigen and possibly even
378 epitope level may be able to resolve different stages of Lyme disease (e.g., acute, acute resolved,
379 PTLD) (10, 60). While the antibody profiling in our study was limited to serum IgG reactivity to
380 OspC, OspC-derived peptides, and VlsE C6-17, the results revealed distinct patterns between the
381 diagnostic and PTLD sample sets when subjected to HC. Most notable was the classification of
382 the C10 peptide: in the diagnostic sample set C10 clustered with C6-17, whereas in the PTLD
383 samples it clustered with the other OspC-derived peptides. Thus, it is tempting to speculate that
384 the ratio of C10 to C6-17 serum IgG reactivity may have some utility in defining disease
385 progression. By the same token, as virtually all samples tested were positive for either C10
386 and/or C6-17, establishing a combined C10 + C6-17 threshold value might serve to alleviate
387 false positives in Lyme disease diagnostics based solely on serology (65, 66). That said we
388 recognize that any claims to this effect are premature, considering that the serum samples
389 employed in our study are not associated with any clinical information beyond seropositivity.
390 Moreover, we lack a "post-Lyme healthy" cohort that Chandra and colleagues so effectively used
391 in their study to compare with their PTLD cohort (10).
392 One interesting grouping that emerged from the PTLD cohort was a cluster of four
393 individuals who demonstrated pan-reactivity with the OspC-derived peptides and VlsE C6-17

394 peptide. In follow-up analysis, those same four samples in question also reacted with other *B.*
395 *burgdorferi*-derived peptides, as well as control non-*B. burgdorferi*-derived peptides, but not
396 necessarily with the corresponding recombinant proteins (G. Freeman-Gallant, unpublished
397 results). Thus, the serum antibodies from those particular individuals seemingly have a
398 propensity for peptide antigens, possibly due to a particular bias in germline chain usage and
399 corresponding paratopes conducive to accommodating peptides (67). Whether or not there is a
400 germline bias in antibodies associated with PTLD is worthy of investigation, especially in light
401 of finding related to COVID-19. Moreover, the availability of bulk plasmablast BCR sequences,
402 as well as single cell paired BCR sequences from LD patients opens the door to detailed antibody
403 reactivity profiles and links to disease manifestations (68). We are also exploring the possibility
404 that these particular samples may have profiles consistent with autoantibodies (69) or have
405 characteristics associated with polyreactivity that might promote ligation to spirochete surface
406 antigens (70, 71).
407
408 **Acknowledgements**
409 We thank Dr. William Lee and other members of the Diagnostic Immunology Laboratory at the
410 Wadsworth Center for providing residual diagnostic serum samples. We gratefully acknowledge
411 Dr. John Martignetti and Lisa Arrigo of the Nuvance Health Lyme disease Biobank for
412 generously providing PTLD serum samples. We thank Elizabeth Cavosie (Wadsworth Center)
413 for administrative assistance and Greta Van Slyke (Wadsworth Center) for establishing Luminex
414 protocols. This work was supported by the National Institute of Allergy and Infectious Diseases
415 (NIAID), National Institutes of Health, Department of Health and Human Services, Contract No.
416 75N93019C00040 (PI/PD Mantis). The content is solely the responsibility of the authors and
417 does not necessarily represent the official views of the National Institutes of Health.
418
419 **Conflicts of Interest**
420 The authors have no conflicts to declare.
421
422 **References Cited**
423
424

1. Kugeler, K. J., A. M. Schwartz, M. J. Delorey, P. S. Mead, and A. F. Hinckley. 2021. Estimating the Frequency of Lyme Disease Diagnoses, United States, 2010-2018. *Emerg Infect Dis* 27: 616-619.
2. Bobe, J. R., B. L. Jutras, E. J. Horn, M. E. Embers, A. Bailey, R. L. Moritz, Y. Zhang, M. J. Soloski, R. S. Ostfeld, R. T. Marconi, J. Aucott, A. Ma'ayan, F. Keesing, K. Lewis, C. Ben Mamoun, A. W. Rebman, M. E. McClune, E. B. Breitschwerdt, P. J. Reddy, R. Maggi, F. Yang, B. Nemser, A. Ozcan, O. Garner, D. Di Carlo, Z. Ballard, H. A. Joung, A. Garcia-Romeu, R. R. Griffiths, N. Baumgarth, and B. A. Fallon. 2021. Recent Progress in Lyme Disease and Remaining Challenges. *Front Med (Lausanne)* 8: 666554.
3. Radolf, J. D., K. Strle, J. E. Lemieux, and F. Strle. 2021. Lyme Disease in Humans. *Curr Issues Mol Biol* 42: 333-384.
4. Steere, A. C., F. Strle, G. P. Wormser, L. T. Hu, J. A. Branda, J. W. Hovius, X. Li, and P. S. Mead. 2016. Lyme borreliosis. *Nat Rev Dis Primers* 2: 16090.
5. Lochhead, R. B., K. Strle, S. L. Arvikar, J. J. Weis, and A. C. Steere. 2021. Lyme arthritis: linking infection, inflammation and autoimmunity. *Nat Rev Rheumatol* 17: 449-461.
6. Klempner, M. S., L. T. Hu, J. Evans, C. H. Schmid, G. M. Johnson, R. P. Trevino, D. Norton, L. Levy, D. Wall, J. McCall, M. Kosinski, and A. Weinstein. 2001. Two controlled trials of antibiotic treatment in patients with persistent symptoms and a history of Lyme disease. *N Engl J Med* 345: 85-92.
7. Marques, A. 2008. Chronic Lyme disease: a review. *Infect Dis Clin North Am* 22: 341-360, vii-viii.
8. Aucott, J. N., L. A. Crowder, and K. B. Kortte. 2013. Development of a foundation for a case definition of post-treatment Lyme disease syndrome. *Int J Infect Dis* 17: e443-449.
9. Aucott, J. N., T. Yang, I. Yoon, D. Powell, S. A. Geller, and A. W. Rebman. 2022. Risk of post-treatment Lyme disease in patients with ideally-treated early Lyme disease: A prospective cohort study. *Int J Infect Dis* 116: 230-237.
10. Chandra, A., G. P. Wormser, A. R. Marques, N. Latov, and A. Alaedini. 2011. Anti-Borrelia burgdorferi antibody profile in post-Lyme disease syndrome. *Clin Vaccine Immunol* 18: 767-771.
11. Blum, L. K., J. Z. Adamska, D. S. Martin, A. W. Rebman, S. E. Elliott, R. R. L. Cao, M. E. Embers, J. N. Aucott, M. J. Soloski, and W. H. Robinson. 2018. Robust B Cell Responses Predict Rapid Resolution of Lyme Disease. *Front Immunol* 9: 1634.
12. Bockenstedt, L. K., R. M. Wooten, and N. Baumgarth. 2021. Immune Response to Borrelia: Lessons from Lyme Disease Spirochetes. *Curr Issues Mol Biol* 42: 145-190.
13. Embers, M. E., N. R. Hasenkampf, M. B. Jacobs, and M. T. Philipp. 2012. Dynamic longitudinal antibody responses during Borrelia burgdorferi infection and antibiotic treatment of rhesus macaques. *Clin Vaccine Immunol* 19: 1218-1226.
14. Jiang, R., H. Meng, K. Raddassi, I. Fleming, K. B. Hoehn, K. R. Dardick, A. A. Belperron, R. R. Montgomery, A. K. Shalek, D. A. Hafler, S. H. Kleinstein, and L. K. Bockenstedt. 2021. Single-cell immunophenotyping of the skin lesion erythema migrans identifies IgM memory B cells. *JCI Insight* 6.
15. Barbour, A. G., A. Jasinskas, M. A. Kayala, D. H. Davies, A. C. Steere, P. Baldi, and P. L. Felgner. 2008. A genome-wide proteome array reveals a limited set of immunogens in natural infections of humans and white-footed mice with Borrelia burgdorferi. *Infect Immun* 76: 3374-3389.

470 16. Tilly, K., J. G. Krum, A. Bestor, M. W. Jewett, D. Grimm, D. Bueschel, R. Byram, D.
471 Dorward, M. J. Vanraden, P. Stewart, and P. Rosa. 2006. Borrelia burgdorferi OspC protein
472 required exclusively in a crucial early stage of mammalian infection. *Infect Immun* 74:
473 3554-3564.
474 17. Pal, U., X. Yang, M. Chen, L. K. Bockenstedt, J. F. Anderson, R. A. Flavell, M. V.
475 Norgard, and E. Fikrig. 2004. OspC facilitates Borrelia burgdorferi invasion of Ixodes
476 scapularis salivary glands. *J Clin Invest* 113: 220-230.
477 18. Tilly, K., A. Bestor, M. W. Jewett, and P. Rosa. 2007. Rapid clearance of Lyme disease
478 spirochetes lacking OspC from skin. *Infect Immun* 75: 1517-1519.
479 19. Earnhart, C. G., D. V. Leblanc, K. E. Alix, D. C. Desrosiers, J. D. Radolf, and R. T.
480 Marconi. 2010. Identification of residues within ligand-binding domain 1 (LBD1) of the
481 Borrelia burgdorferi OspC protein required for function in the mammalian environment.
482 *Mol Microbiol* 76: 393-408.
483 20. Caine, J. A., and J. Coburn. 2016. Multifunctional and Redundant Roles of Borrelia
484 burgdorferi Outer Surface Proteins in Tissue Adhesion, Colonization, and Complement
485 Evasion. *Front Immunol* 7: 442.
486 21. Caine, J. A., Y. P. Lin, J. R. Kessler, H. Sato, J. M. Leong, and J. Coburn. 2017. Borrelia
487 burgdorferi outer surface protein C (OspC) binds complement component C4b and confers
488 bloodstream survival. *Cell Microbiol* 19.
489 22. Lin, Y. P., X. Tan, J. A. Caine, M. Castellanos, G. Chaconas, J. Coburn, and J. M. Leong.
490 2020. Strain-specific joint invasion and colonization by Lyme disease spirochetes is
491 promoted by outer surface protein C. *PLoS Pathog* 16: e1008516.
492 23. Tan, X., M. Castellanos, and G. Chaconas. 2023. Choreography of Lyme Disease
493 Spirochete Adhesins To Promote Vascular Escape. *Microbiol Spectr* 11: e0125423.
494 24. Branda, J. A., and A. C. Steere. 2021. Laboratory Diagnosis of Lyme Borreliosis. *Clin*
495 *Microbiol Rev* 34.
496 25. Hahm, J. B., J. W. t. Breneman, J. Liu, S. Rabkina, W. Zheng, S. Zhou, R. P. Walker, and
497 R. Kaul. 2020. A Fully Automated Multiplex Assay for Diagnosis of Lyme Disease with
498 High Specificity and Improved Early Sensitivity. *J Clin Microbiol* 58.
499 26. Bacon, R. M., B. J. Biggerstaff, M. E. Schriefer, R. D. Gilmore, Jr., M. T. Philipp, A. C.
500 Steere, G. P. Wormser, A. R. Marques, and B. J. Johnson. 2003. Serodiagnosis of Lyme
501 disease by kinetic enzyme-linked immunosorbent assay using recombinant VlsE1 or
502 peptide antigens of Borrelia burgdorferi compared with 2-tiered testing using whole-cell
503 lysates. *J Infect Dis* 187: 1187-1199.
504 27. Arnaboldi, P. M., R. Seedarnee, M. Sambir, S. M. Callister, J. A. Imparato, and R. J.
505 Dattwyler. 2013. Outer surface protein C peptide derived from Borrelia burgdorferi sensu
506 stricto as a target for serodiagnosis of early lyme disease. *Clin Vaccine Immunol* 20: 474-
507 481.
508 28. Baarsma, M. E., A. Vrijlandt, J. Ursinus, H. L. Zaaijer, S. Jurriaans, A. P. van Dam, and J.
509 W. Hovius. 2022. Diagnostic performance of the ZEUS Borrelia VlsE1/pepC10 assay in
510 European LB patients: a case-control study. *Eur J Clin Microbiol Infect Dis* 41: 387-393.
511 29. Coleman, A. S., E. Rossmann, X. Yang, H. Song, C. M. Lamichhane, R. Iyer, I. Schwartz,
512 and U. Pal. 2011. BBK07 immunodominant peptides as serodiagnostic markers of Lyme
513 disease. *Clin Vaccine Immunol* 18: 406-413.

514 30. Mathiesen, M. J., M. Christiansen, K. Hansen, A. Holm, E. Asbrink, and M. Theisen. 1998.
515 Peptide-based OspC enzyme-linked immunosorbent assay for serodiagnosis of Lyme
516 borreliosis. *J Clin Microbiol* 36: 3474-3479.
517 31. O'Bier, N. S., A. L. Hatke, A. C. Camire, and R. T. Marconi. 2021. Human and Veterinary
518 Vaccines for Lyme Disease. *Curr Issues Mol Biol* 42: 191-222.
519 32. Wilske, B., V. Preac-Mursic, S. Jauris, A. Hofmann, I. Pradel, E. Soutschek, E. Schwab,
520 G. Will, and G. Wanner. 1993. Immunological and molecular polymorphisms of OspC, an
521 immunodominant major outer surface protein of Borrelia burgdorferi. *Infect Immun* 61:
522 2182-2191.
523 33. Barbour, A. G., and B. Travinsky. 2010. Evolution and distribution of the ospC Gene, a
524 transferable serotype determinant of Borrelia burgdorferi. *MBio* 1.
525 34. Cerar, T., F. Strle, D. Stupica, E. Ruzic-Sabljic, G. McHugh, A. C. Steere, and K. Strle.
526 2016. Differences in Genotype, Clinical Features, and Inflammatory Potential of Borrelia
527 burgdorferi sensu stricto Strains from Europe and the United States. *Emerg Infect Dis* 22:
528 818-827.
529 35. Seinost, G., D. E. Dykhuizen, R. J. Dattwyler, W. T. Golde, J. J. Dunn, I. N. Wang, G. P.
530 Wormser, M. E. Schriefer, and B. J. Luft. 1999. Four clones of Borrelia burgdorferi sensu
531 stricto cause invasive infection in humans. *Infect Immun* 67: 3518-3524.
532 36. Earnhart, C. G., E. L. Buckles, J. S. Dumler, and R. T. Marconi. 2005. Demonstration of
533 OspC type diversity in invasive human lyme disease isolates and identification of
534 previously uncharacterized epitopes that define the specificity of the OspC murine antibody
535 response. *Infect Immun* 73: 7869-7877.
536 37. Hanincova, K., P. Mukherjee, N. H. Ogden, G. Margos, G. P. Wormser, K. D. Reed, J. K.
537 Meece, M. F. Vandermause, and I. Schwartz. 2013. Multilocus sequence typing of Borrelia
538 burgdorferi suggests existence of lineages with differential pathogenic properties in
539 humans. *PLoS One* 8: e73066.
540 38. Fraser, C. M., S. Casjens, W. M. Huang, G. G. Sutton, R. Clayton, R. Lathigra, O. White,
541 K. A. Ketchum, R. Dodson, E. K. Hickey, M. Gwinn, B. Dougherty, J. F. Tomb, R. D.
542 Fleischmann, D. Richardson, J. Peterson, A. R. Kerlavage, J. Quackenbush, S. Salzberg,
543 M. Hanson, R. van Vugt, N. Palmer, M. D. Adams, J. Gocayne, J. Weidman, T. Utterback,
544 L. Watthey, L. McDonald, P. Artiach, C. Bowman, S. Garland, C. Fuji, M. D. Cotton, K.
545 Horst, K. Roberts, B. Hatch, H. O. Smith, and J. C. Venter. 1997. Genomic sequence of a
546 Lyme disease spirochaete, Borrelia burgdorferi. *Nature* 390: 580-586.
547 39. Anderson, J. F., R. A. Flavell, L. A. Magnarelli, S. W. Barthold, F. S. Kantor, R. Wallich,
548 D. H. Persing, D. Mathiesen, and E. Fikrig. 1996. Novel Borrelia burgdorferi isolates from
549 Ixodes scapularis and Ixodes dentatus ticks feeding on humans. *J Clin Microbiol* 34: 524-
550 529.
551 40. Steere, A. C., R. L. Grodzicki, A. N. Kornblatt, J. E. Craft, A. G. Barbour, W. Burgdorfer,
552 G. P. Schmid, E. Johnson, and S. E. Malawista. 1983. The spirochetal etiology of Lyme
553 disease. *N Engl J Med* 308: 733-740.
554 41. Rudolph, M. J., S. A. Davis, H. M. E. Haque, D. D. Weis, D. J. Vance, C. L. Piazza, M.
555 Ejemel, L. Cavacini, Y. Wang, M. L. Mbow, R. D. Gilmore, and N. J. Mantis. 2023.
556 Structural Elucidation of a Protective B Cell Epitope on Outer Surface Protein C (OspC)
557 of the Lyme Disease Spirochete, Borreliella burgdorferi. *mBio* 14: e0298122.

42. Kringelum, J. V., C. Lundegaard, O. Lund, and M. Nielsen. 2012. Reliable B cell epitope predictions: impacts of method development and improved benchmarking. *PLoS Comput Biol* 8: e1002829.
43. Gomes-Solecki, M. J., L. Meirelles, J. Glass, and R. J. Dattwyler. 2007. Epitope length, genospecies dependency, and serum panel effect in the IR6 enzyme-linked immunosorbent assay for detection of antibodies to Borrelia burgdorferi. *Clin Vaccine Immunol* 14: 875-879.
44. Nemeth, K. L., E. Yauney, J. M. Rock, R. Bievenue, M. M. Parker, and L. M. Styer. 2023. Use of Self-Collected Dried Blood Spots and a Multiplex Microsphere Immunoassay to Measure IgG Antibody Response to COVID-19 Vaccines. *Microbiol Spectr* 11: e0133622.
45. Yates, J. L., D. J. Ehrbar, D. T. Hunt, R. C. Girardin, A. P. Dupuis, A. F. Payne, M. Sowizral, S. Varney, K. E. Kulas, V. L. Demarest, K. M. Howard, K. Carson, M. Hales, M. Ejemel, Q. Li, Y. Wang, R. Peredo-Wende, A. Ramani, G. Singh, K. Strle, N. J. Mantis, K. A. McDonough, and W. T. Lee. 2021. Serological Analysis Reveals an Imbalanced IgG Subclass Composition Associated with COVID-19 Disease Severity. *Cell Reports Medicine*: 100329.
46. R core Team. 2023. R: A language and environment for statistical computing. *R Foundation for Statistical Computing,*.
47. Wickham, H., and J. Bryan. 2023. Read Excel Files. 1.4.3 ed, CRAN. Import excel files into R. Supports '.xls' via the embedded

'libxls' C library <https://github.com/libxls/libxls> and '.xlsx' via

the embedded 'RapidXML' C++ library <https://rapidxml.sourceforge.net/>.

Works on Windows, Mac and Linux without external dependencies.
48. Wickham, H. 2019. Welcome to the Tidyverse. *Journal of Open Source Software* 4: 1686.
49. Wei, T., V. Simko, M. Levy, Y. Xie, Y. Jin, and J. Zemla. 2017. Package 'corrplot'. *Statistician* 56: e24.
50. Kolde, R. 2018. pheatmap: Pretty Heatmaps.
51. Lemieux, J. E., W. Huang, N. Hill, T. Cerar, L. Freimark, S. Hernandez, M. Luban, V. Maraspin, P. Bogovic, K. Ogrinc, E. Ruzic-Sabljic, P. Lapierre, E. Lasek-Nesselquist, N. Singh, R. Iyer, D. Liveris, K. D. Reed, J. M. Leong, J. A. Branda, A. C. Steere, G. P. Wormser, F. Strle, P. C. Sabeti, I. Schwartz, and K. Strle. 2023. Whole genome sequencing of human Borrelia burgdorferi isolates reveals linked blocks of accessory genome elements located on plasmids and associated with human dissemination. *PLoS Pathog* 19: e1011243.
52. Wormser, G. P., D. Brisson, D. Liveris, K. Hanincova, S. Sandigursky, J. Nowakowski, R. B. Nadelman, S. Ludin, and I. Schwartz. 2008. Borrelia burgdorferi genotype predicts the capacity for hematogenous dissemination during early Lyme disease. *J Infect Dis* 198: 1358-1364.
53. Dimitrov, J. D., C. Planchais, L. T. Roumenina, T. L. Vassilev, S. V. Kaveri, and S. Lacroix-Desmazes. 2013. Antibody polyreactivity in health and disease: statu variabilis. *J Immunol* 191: 993-999.
54. Mathiesen, M. J., A. Holm, M. Christiansen, J. Blom, K. Hansen, S. Ostergaard, and M. Theisen. 1998. The dominant epitope of Borrelia garinii outer surface protein C recognized by sera from patients with neuroborreliosis has a surface-exposed conserved structural motif. *Infect Immun* 66: 4073-4079.

602 55. Earnhart, C. G., D. V. Rhodes, A. A. Smith, X. Yang, B. Tegels, J. A. Carlyon, U. Pal, and
603 R. T. Marconi. 2014. Assessment of the potential contribution of the highly conserved C-
604 terminal motif (C10) of Borrelia burgdorferi outer surface protein C in transmission and
605 infectivity. *Pathog Dis* 70: 176-184.
606 56. Dolange, V., S. Simon, and N. Morel. 2021. Detection of Borrelia burgdorferi antigens in
607 tissues and plasma during early infection in a mouse model. *Sci Rep* 11: 17368.
608 57. Jobe, D. A., S. D. Lovrich, R. F. Schell, and S. M. Callister. 2003. C-terminal region of
609 outer surface protein C binds borreliacidal antibodies in sera from patients with Lyme
610 disease. *Clin Diagn Lab Immunol* 10: 573-578.
611 58. Lovrich, S. D., D. A. Jobe, R. F. Schell, and S. M. Callister. 2005. Borreliacidal OspC
612 antibodies specific for a highly conserved epitope are immunodominant in human lyme
613 disease and do not occur in mice or hamsters. *Clin Diagn Lab Immunol* 12: 746-751.
614 59. Izac, J. R., A. C. Camire, C. G. Earnhart, M. E. Embers, R. A. Funk, E. B. Breitschwerdt,
615 and R. T. Marconi. 2019. Analysis of the antigenic determinants of the OspC protein of the
616 Lyme disease spirochetes: Evidence that the C10 motif is not immunodominant or required
617 to elicit bactericidal antibody responses. *Vaccine* 37: 2401-2407.
618 60. Jacek, E., K. S. Tang, L. Komorowski, M. Ajamian, C. Probst, B. Stevenson, G. P.
619 Wormser, A. R. Marques, and A. Alaedini. 2016. Epitope-Specific Evolution of Human B
620 Cell Responses to Borrelia burgdorferi VlsE Protein from Early to Late Stages of Lyme
621 Disease. *J Immunol* 196: 1036-1043.
622 61. Kirpach, J., A. Colone, J. P. Burckert, W. J. Faison, A. Dubois, R. Sinner, A. L. Reye, and
623 C. P. Muller. 2019. Detection of a Low Level and Heterogeneous B Cell Immune Response
624 in Peripheral Blood of Acute Borreliosis Patients With High Throughput Sequencing.
625 *Front Immunol* 10: 1105.
626 62. Hoie, M. H., F. S. Gade, J. M. Johansen, C. Wurtzen, O. Winther, M. Nielsen, and P.
627 Marcatili. 2024. DiscoTope-3.0: improved B-cell epitope prediction using inverse folding
628 latent representations. *Front Immunol* 15: 1322712.
629 63. Buckles, E. L., C. G. Earnhart, and R. T. Marconi. 2006. Analysis of antibody response in
630 humans to the type A OspC loop 5 domain and assessment of the potential utility of the
631 loop 5 epitope in Lyme disease vaccine development. *Clin Vaccine Immunol* 13: 1162-
632 1165.
633 64. Yang, X., Y. Li, J. J. Dunn, and B. J. Luft. 2006. Characterization of a unique borreliacidal
634 epitope on the outer surface protein C of Borrelia burgdorferi. *FEMS Immunol Med*
635 *Microbiol* 48: 64-74.
636 65. Rebman, A. W., L. A. Crowder, A. Kirkpatrick, and J. N. Aucott. 2015. Characteristics of
637 seroconversion and implications for diagnosis of post-treatment Lyme disease syndrome:
638 acute and convalescent serology among a prospective cohort of early Lyme disease
639 patients. *Clin Rheumatol* 34: 585-589.
640 66. Reifert, J., K. Kamath, J. Bozekowski, E. Lis, E. J. Horn, D. Granger, E. S. Theel, J. Shon,
641 J. R. Sawyer, and P. S. Daugherty. 2021. Serum Epitope Repertoire Analysis Enables Early
642 Detection of Lyme Disease with Improved Sensitivity in an Expandable Multiplex Format.
643 *J Clin Microbiol* 59.
644 67. Cobaugh, C. W., J. C. Almagro, M. Pogson, B. Iverson, and G. Georgiou. 2008. Synthetic
645 antibody libraries focused towards peptide ligands. *J Mol Biol* 378: 622-633.

646 68. Blum, J. S., M. L. Fiani, and P. D. Stahl. 1991. Proteolytic cleavage of ricin A chain in
647 endosomal vesicles. Evidence for the action of endosomal proteases at both neutral and
648 acidic pH. *J Biol Chem* 266: 22091-22095.
649 69. Trier, N. H., and G. Houen. 2023. Antibody Cross-Reactivity in Auto-Immune Diseases.
650 *Int J Mol Sci* 24.
651 70. Boughter, C. T., M. T. Borowska, J. J. Guthmiller, A. Bendelac, P. C. Wilson, B. Roux,
652 and E. J. Adams. 2020. Biochemical patterns of antibody polyreactivity revealed through
653 a bioinformatics-based analysis of CDR loops. *Elife* 9.
654 71. Mouquet, H., J. F. Scheid, M. J. Zoller, M. Krogsgaard, R. G. Ott, S. Shukair, M. N.
655 Artyomov, J. Pietzsch, M. Connors, F. Pereyra, B. D. Walker, D. D. Ho, P. C. Wilson, M.
656 S. Seaman, H. N. Eisen, A. K. Chakraborty, T. J. Hope, J. V. Ravetch, H. Wardemann, and
657 M. C. Nussenzweig. 2010. Polyreactivity increases the apparent affinity of anti-HIV
658 antibodies by heteroligation. *Nature* 467: 591-595.
659 72. Ikushima, M., F. Yamada, S. Kawahashi, Y. Okuyama, and K. Matsui. 1999. Antibody
660 response to OspC-I synthetic peptide derived from outer surface protein C of Borrelia
661 burgdorferi in sera from Japanese forestry workers. *Epidemiol Infect* 122: 429-433.
662 73. Pulzova, L., Z. Flachbartova, E. Bencurova, L. Potocnakova, L. Comor, E. Schreterova,
663 and M. Bhide. 2016. Identification of B-cell epitopes of Borrelia burgdorferi outer surface
664 protein C by screening a phage-displayed gene fragment library. *Microbiol Immunol* 60:
665 669-677.
666 74. Tokarz, R., N. Mishra, T. Tagliafierro, S. Sameroff, A. Caciula, L. Chauhan, J. Patel, E.
667 Sullivan, A. Gucwa, B. Fallon, M. Golightly, C. Molins, M. Schriefer, A. Marques, T.
668 Briese, and W. I. Lipkin. 2018. A multiplex serologic platform for diagnosis of tick-borne
669 diseases. *Sci Rep* 8: 3158.
670 75. Yu, Z., J. M. Carter, L. H. Sigal, and S. Stein. 1996. Multi-well ELISA based on
671 independent peptide antigens for antibody capture. Application to Lyme disease
672 serodiagnosis. *J Immunol Methods* 198: 25-33.
673 76. Baum, E., A. Z. Randall, M. Zeller, and A. G. Barbour. 2013. Inferring epitopes of a
674 polymorphic antigen amidst broadly cross-reactive antibodies using protein microarrays: a
675 study of OspC proteins of Borrelia burgdorferi. *PLoS One* 8: e67445.

676

677

678 **FIGURE LEGENDS**

679

680 **Figure 1. Relative location of linear epitopes on homodimeric $OspC_A$.** (**A**) Surface
681 representation of homodimeric $OspC_A$ (residues 38-201; PDB 1GGQ] with one monomer
682 (OspC) colored gray and the other, denoted with an apostrophe (OspC'), colored in charcoal. The
683 linear epitopes examined in this study are coded and numbered according to **Table 1**. Epitope 1
684 is represented as a bracket (]) on OspC', as its corresponding residues were truncated in the
685 recombinant version of $OspC_A$ used for X-ray crystal structure analysis. Similarly, only residues
686 193-201 of epitope 8 (residues 193-210) are shown because the C-terminus of $OspC_A$ was
687 truncated at position 201. Overlap between epitopes 6 and 7 are colored as epitope 6. (**B**) The
688 same image as Panel A except that amino acid differences between OspC types A, B and K
689 within the eight epitopes are colored red to illustrate degree of polymorphisms.

690

691 **Figure 2. Serum IgG reactivity of diagnostic and PTLD samples with OspC and OspC-**
692 **derived peptides.** (**A**) DI and (**B**) PTLD serum samples (diluted 1:100) were subject to MIA
693 using microspheres coated with recombinant dimeric OspC types A, B and K (top rows), OspC-
694 peptides as described in Table 1, and C6-17 peptide. Panels are labeled by corresponding residue
695 numbers for each OspC type. MFI values were $log_{10}$ transformed and compared to the control
696 sample set. Significance was determined by the Mann-Whitney U-test (*, $p < 0.05$).

697

698 **Figure 3. Indexed (>6SD) IgG reactivity of DI and PTLD serum samples with OspC and**
699 **OspC-derived peptides.** MFI values for OspC and OspC- and VlsE-derived peptides were
700 indexed using a cutoff of 6SD above mean control reactivity. The resulting values were then
701 $log_{10}$ transformed with each point representing a single sample. OspC subtypes are listed along
702 the x-axis, residues are indicated along the top of the plot (**B**, **D**), and each antigen is represented
703 by a different color. In each of the graphs, the 6 SD cutoff corresponds to a value of 0 on the y-
704 axis and is depicted with horizontal red line. All samples falling above y = 0 were found to be
705 positive for the given antigen and were used to calculate percent positivity and fold increase as
706 reported in Tables 2 and 3. Box and whisker plots illustrate the upper and lower quartiles as well

707 as the median reactivity to each antigen (thick center line). Sample points that fall above or
708 below the whiskers are considered outliers. Violin plots outline the distribution of data.
709
710 **Figure 4. Correlation matrices of rOspC and OspC-derived peptide reactivity in diagnostic**
711 **and PTLD serum.** Diagnostic (**A**) and PTLD (**B**) serum sample MFIs (indexed and $\log_{10}$
712 transformed) were subjected to Spearman's Rank correlation. Only significant correlation
713 coefficients ($r_s$) are displayed (confidence level = 0.95). The degree and direction of correlation is
714 indicated by the color scale. Interpretations of the strength of each correlation was conducted as
715 such: >0.7 indicates a strong correlation, 0.5 – 0.7 is moderate, 0.3 – 0.5 is weak, and 0.0 – 0.3 is
716 negligible.
717
718 **Figure 5. Hierarchical clustering of rOspC and OspC-derived reactivity in diagnostic and**
719 **PTLD serum.** Heatmaps were generated using diagnostic (**A**) and PTLD (**B**) serum sample MFIs
720 (indexed and $\log_{10}$ transformed). Rows represent individual samples and columns represent the
721 panel of antigens. The color scales of **A** and B are identical to one another (allowing for direct
722 comparison), with 0 representing the positivity cutoff (as seen in **Figure 3**). Annotation of the
723 diagnostic samples (**A**) with Western blot profile data (previously described in the Materials and
724 Methods) is designated by the legend. The columns were subjected to hierarchical clustering by
725 correlation and the rows were clustered by Euclidean distance to better visualize patterns in
726 reactivity profiles.
727
728 **Figure 6: Correlation between $OspC_A$ reactivity and C10 region.** Diagnostic (n=686) and
729 PTLD (n=158) samples were subjected to Luminex with $OspC_A$, $OspC_A$+C10, and $193\text{-}210_A$ as
730 described in the Materials and Methods. $OspC_A$ MFIs were evaluated against $OspC_A$+C10 for
731 diagnostic **(A)** and PTLD **(D)** samples. Significance was determined by Mann-Whitney U test. *,
732 $p < 0.05$. To examine the contribution of the C10 region to $OspC_A$ reactivity, MFIs for peptide
733 $193\text{-}210_A$ were plotted (on the y-axis) versus MFIs from $OspC_A$ and $OspC_A$+C10 (on the x-axis)
734 for diagnostic samples **(B, C)** and PTLD samples **(E, F)**. Best fit lines and confidence intervals
735 (level = 0.95) were added to each plot using a linear regression model. Adjusted R-squared ($r^2$)
736 values were calculated in R.

737 **TABLES**

738

**Table 1. OspC and VlsE-derived peptides used in this study**

| #[a] | residues | OspC type sequence | IEDB ID [b] | References |
|---|---|---|---|---|
| **1** | 9-33 | ILMTLFLFISCNNSGKDGNTSANSA | 181204<br>745120 | (72)<br>(27)<br>(73)<br>(74) |
| **2** | 40-55 | A/B–PNLTEISKKITDSNAV<br>K–PNLTEISKKITESNAV | 559957 | (73) |
| **3** | 71-86 | A–EIAAKAIGKKIHQNNG | 12383 | (75) |
| **4** | 132-146<br>132-146<br>133-147 | A–ETFTNKLKEKHTDLG<br>B–EEFSTKLKDNHAQLG<br>K–EDFTKKLEGEHAQLG | 63756 ,745097<br>14380, 18025 | (64) |
| **5** | 155-169 | A–AKEAILKTNGTKTKG | 558968<br>181187 | (27)<br>(73) |
| **6** | 177-186<br>178-187<br>178-187 | A–FESVEVLSKA<br>B–SGSLESLSKA<br>K–FKAVENLAKA | NA | (76) |
| **7** | 183-190[c] | A/B–LSKAAKEM | 560173 | (73) |
| **8** | 193-210 | A–NSVKELTSPVVAESPKKP | 745122 | (25, 54, 73, 74) |
| **C6** | VlsE C6-17 | MKKDDQIAAAIALRGMA | 41843 | (43) |

[a], Numbers correspond to peptides highlighted in Figure 1, except C6. [b], Immune Epitope Database (IEDB.org) identifier. [c], Residues 184-191 in Type B.

739

740

741

742

**Table 2: Serum IgG reactivity > 6SD to $OspC_{A/B/K}$ and OspC peptides in diagnostic and PTLD serum samples**

| | Diagnostic | | PTLD | |
|---|---|---|---|---|
| **OspC or peptide** | **n = (%)[a]** | **Fold increase (SD)[b]** | **n = (%)[a]** | **Fold increase (SD)[b]** |
| $OspC_A$ | 167 (24.0) | 2.8 (1.9) | 29 (18.4) | 5.5 (5.6) |
| $OspC_B$ | 287 (41.2) | 3.7 (3.4) | 5 (3.2) | 2.1 (0.6) |
| $OspC_K$ | 195 (28.0) | 4.7 (4.3) | 26 (16.5) | 2.8 (2.2) |
| $9\text{-}33_{ABK}$ | 1 (0.1) | 2.4 (N/A) | 0 (0) | N/A (N/A) |
| $40\text{-}55_{AB}$ | 17 (2.4) | 2.1 (1.4) | 4 (2.5) | 1.6 (0.5) |
| $40\text{-}55_K$ | 7 (1.0) | 1.5 (0.5) | 2 (1.3) | 1.3 (0.2) |
| $71\text{-}86_A$ | 28 (4.0) | 1.7 (0.8) | 1 (0.6) | 1.4 (NA) |
| $132\text{-}146_A$ | 18 (2.6) | 2.4 (1.5) | 5 (3.2) | 1.7 (0.6) |
| $132\text{-}146_B$ | 48 (6.9) | 2.0 (1.3) | 11 (7.0) | 3.0 (1.9) |
| $133\text{-}147_K$ | 36 (5.2) | 2.4 (2.6) | 8 (5.1) | 2.5 (1.2) |
| $155\text{-}169_A$ | 30 (4.3) | 2.5 (2.5) | 5 (3.2) | 2.5 (1.5) |
| $177\text{-}186_A$ | 38 (5.5) | 1.6 (0.7) | 13 (8.2) | 2.6 (2.0) |
| $178\text{-}187_K$ | 70 (10.1) | 1.5 (0.7) | 15 (9.5) | 3.0 (2.8) |
| $178\text{-}187_B$ | 7 (1.0) | 1.2 (0.1) | 12 (7.6) | 2.7 (1.9) |
| $183\text{-}190_{AB}$[c] | 53 (7.6) | 1.9 (1.0) | 14 (8.9) | 3.0 (3.1) |
| $193\text{-}210_A$ (C10) | 185 (26.6) | 4.4 (4.5) | 22 (14.0) | 3.3 (3.0) |
| VlsE C6-17 | 496 (71.3) | 5.8 (2.9) | 64 (40.5) | 5.6 (5.0) |

[a], The number of samples (n =) and percent reactivity ("%") to each antigen in the Diagnostic (n=696) and PTLD (n=158) sample sets were calculated using a cutoff of >6SD above the mean of controls samples; [b], The fold increase (magnitude) of positive sample antibody reactivity over controls such than an index value of 1 is 6SD above the control mean, while 2.8 corresponds to ~16SD greater than the mean control. [c], $OspC_B$ residues 184-191.

743

744

**Figure 1**

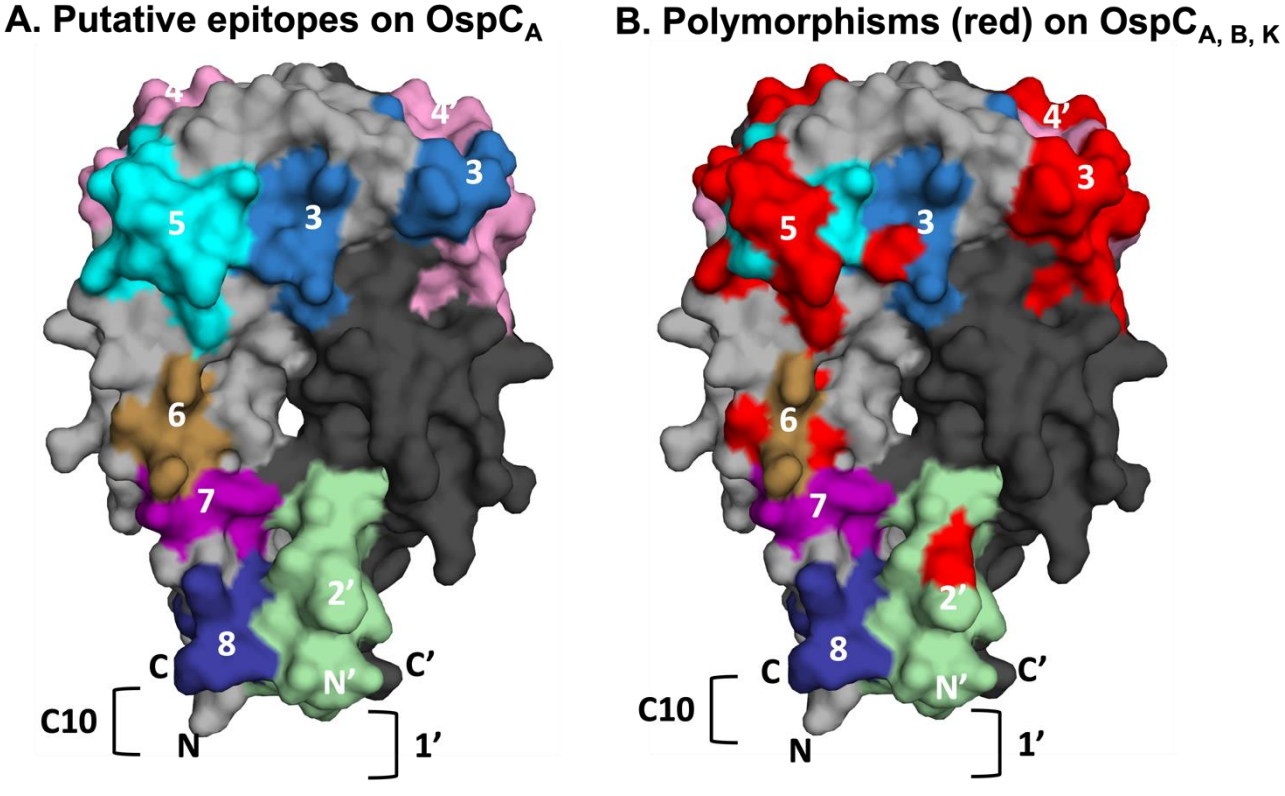
A. Putative epitopes on OspC$_A$
B. Polymorphisms (red) on OspC$_{A, B, K}$
4
4'
3
5
3
6
7
2'
8
C
N'
C'
C10
N
1'

# Figure 2

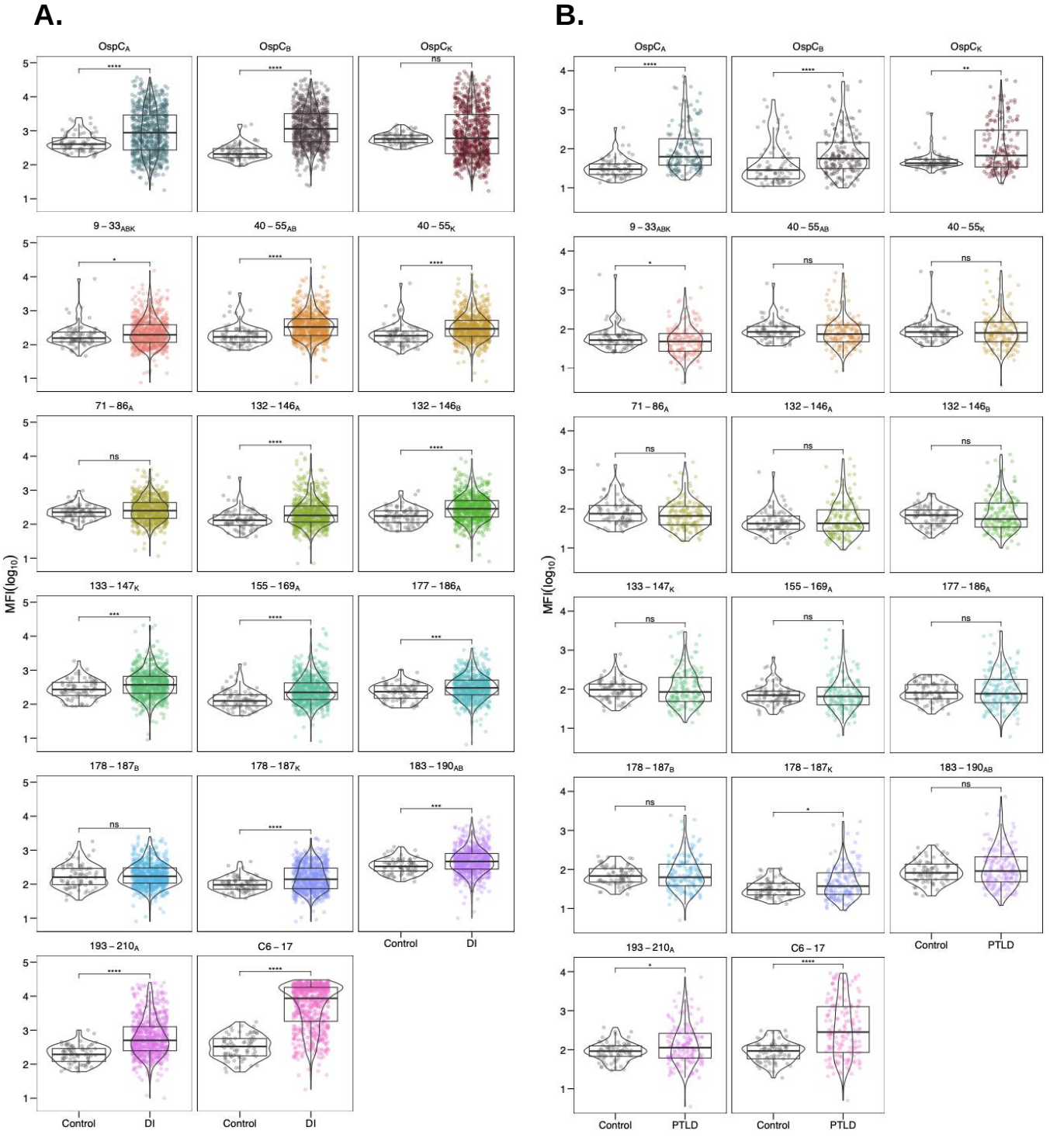
A.
B.
MFI(log10)
OspCA
OspCB
OspCK
9 – 33ABK
40 – 55AB
40 – 55K
71 – 86A
132 – 146A
132 – 146B
133 – 147K
155 – 169A
177 – 186A
178 – 187B
178 – 187K
183 – 190AB
193 – 210A
C6 – 17
Control
DI
PTLD

# Figure 3

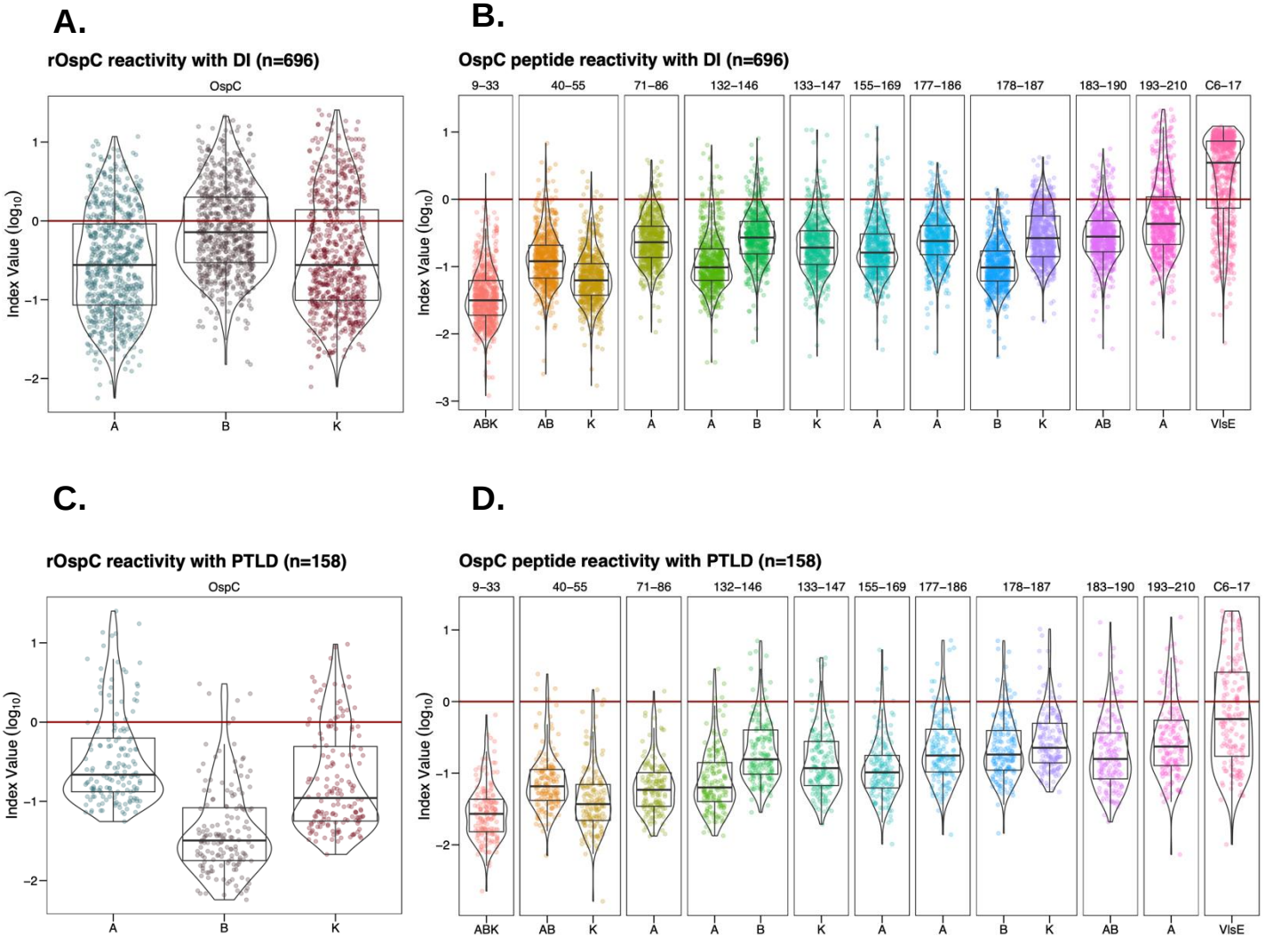
A.
rOspC reactivity with DI (n=696)
OspC
Index Value (log10)
A
B
K
B.
OspC peptide reactivity with DI (n=696)
9–33
40–55
71–86
132–146
133–147
155–169
177–186
178–187
183–190
193–210
C6–17
ABK
AB
K
A
A
B
K
A
A
B
K
AB
A
VlsE
C.
rOspC reactivity with PTLD (n=158)
D.
OspC peptide reactivity with PTLD (n=158)

# Figure 4

**A.**

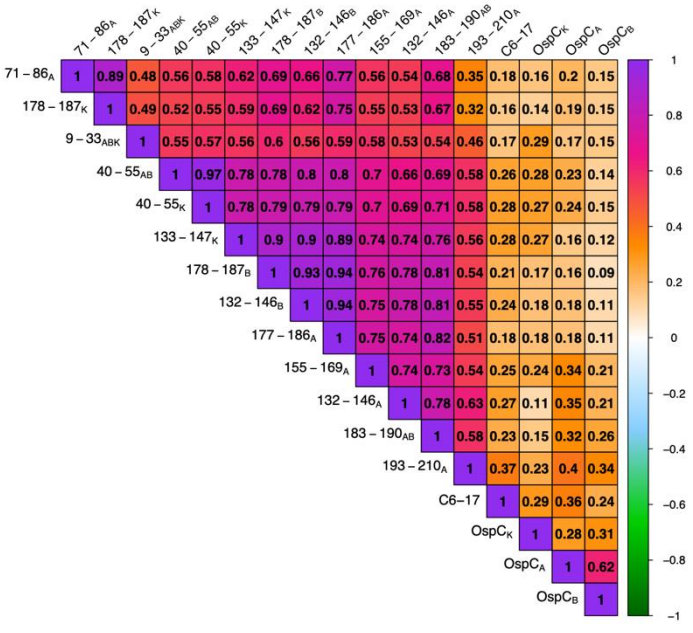
71 – 86A
178 – 187K
9 – 33ABK
40 – 55AB
40 – 55K
133 – 147K
178 – 187B
132 – 146B
177 – 186A
155 – 169A
132 – 146A
183 – 190AB
193 – 210A
C6–17
OspCK
OspCA
OspCB
1 0.89 0.48 0.56 0.58 0.62 0.69 0.66 0.77 0.56 0.54 0.68 0.35 0.18 0.16 0.2 0.15
1 0.49 0.52 0.55 0.59 0.69 0.62 0.75 0.55 0.53 0.67 0.32 0.16 0.14 0.19 0.15
1 0.55 0.57 0.56 0.6 0.56 0.59 0.58 0.53 0.54 0.46 0.17 0.29 0.17 0.15
1 0.97 0.78 0.78 0.8 0.8 0.7 0.66 0.69 0.58 0.26 0.28 0.23 0.14
1 0.78 0.79 0.79 0.79 0.7 0.69 0.71 0.58 0.28 0.27 0.24 0.15
1 0.9 0.9 0.89 0.74 0.74 0.76 0.56 0.28 0.27 0.16 0.12
1 0.93 0.94 0.76 0.78 0.81 0.54 0.21 0.17 0.16 0.09
1 0.94 0.75 0.78 0.81 0.55 0.24 0.18 0.18 0.11
1 0.75 0.74 0.82 0.51 0.18 0.18 0.18 0.11
1 0.74 0.73 0.54 0.25 0.24 0.34 0.21
1 0.78 0.63 0.27 0.11 0.35 0.21
1 0.58 0.23 0.15 0.32 0.26
1 0.37 0.23 0.4 0.34
1 0.29 0.36 0.24
1 0.28 0.31
1 0.62
1
1
0.8
0.6
0.4
0.2
0
−0.2
−0.4
−0.6
−0.8
−1

**B.**

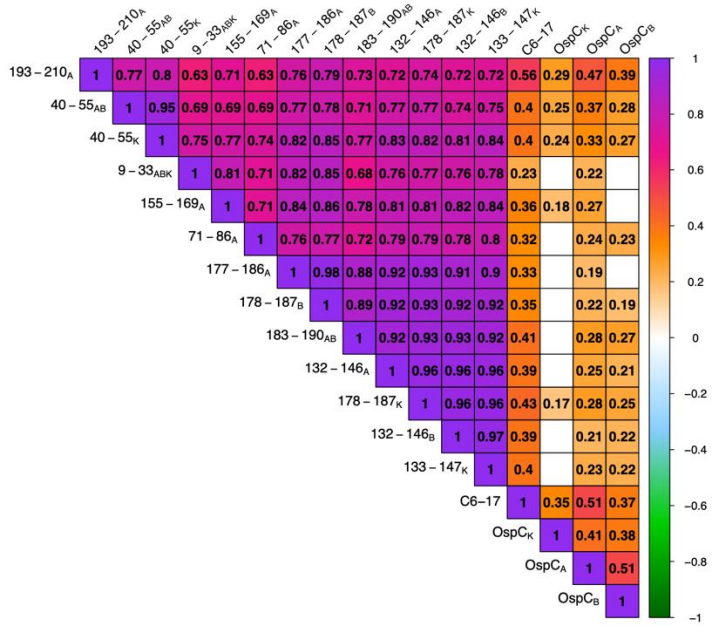
193 – 210A
40 – 55AB
40 – 55K
9 – 33ABK
155 – 169A
71 – 86A
177 – 186A
178 – 187B
183 – 190AB
132 – 146A
178 – 187K
132 – 146B
133 – 147K
C6–17
OspCK
OspCA
OspCB
1 0.77 0.8 0.63 0.71 0.63 0.76 0.79 0.73 0.72 0.74 0.72 0.72 0.56 0.29 0.47 0.39
1 0.95 0.69 0.69 0.69 0.77 0.78 0.71 0.77 0.77 0.74 0.75 0.4 0.25 0.37 0.28
1 0.75 0.77 0.74 0.82 0.85 0.77 0.83 0.82 0.81 0.84 0.4 0.24 0.33 0.27
1 0.81 0.71 0.82 0.85 0.68 0.76 0.77 0.76 0.78 0.23 0.22
1 0.71 0.84 0.86 0.78 0.81 0.81 0.82 0.84 0.36 0.18 0.27
1 0.76 0.77 0.72 0.79 0.79 0.78 0.8 0.32 0.24 0.23
1 0.98 0.88 0.92 0.93 0.91 0.9 0.33 0.19
1 0.89 0.92 0.93 0.92 0.92 0.35 0.22 0.19
1 0.92 0.93 0.93 0.92 0.41 0.28 0.27
1 0.96 0.96 0.96 0.39 0.25 0.21
1 0.96 0.96 0.43 0.17 0.28 0.25
1 0.97 0.39 0.21 0.22
1 0.4 0.23 0.22
1 0.35 0.51 0.37
1 0.41 0.38
1 0.51
1
1
0.8
0.6
0.4
0.2
0
−0.2
−0.4
−0.6
−0.8
−1

Figure 5

A.

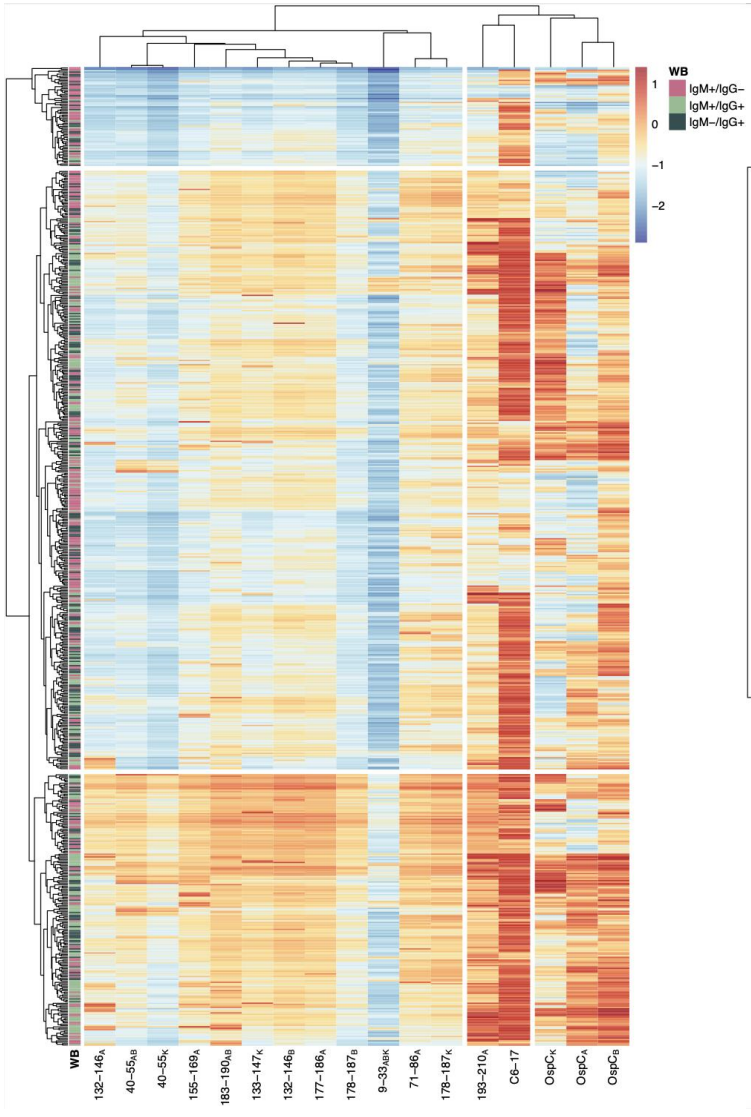
WB
IgM+/IgG−
IgM+/IgG+
IgM−/IgG+
1
0
−1
−2
WB
132–146A
40–55AB
40–55K
155–169A
183–190AB
133–147K
132–146B
177–186A
178–187B
9–33ABK
71–86A
178–187K
193–210A
C6–17
OspCK
OspCA
OspCB

B.

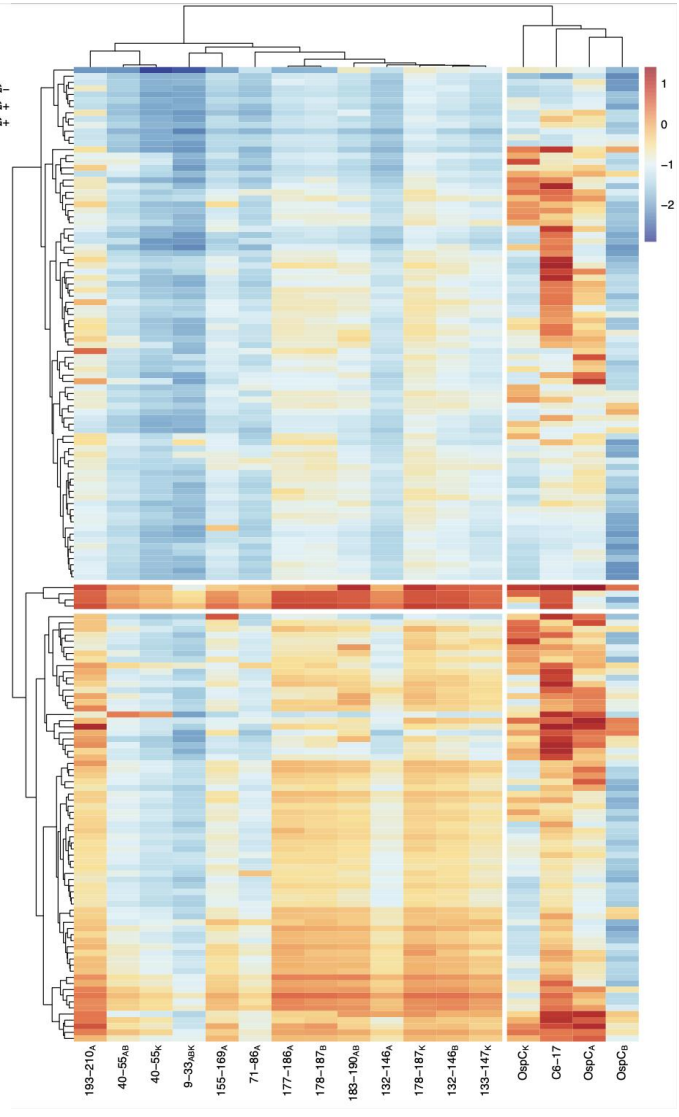
1
0
−1
−2
193–210A
40–55AB
40–55K
9–33ABK
155–169A
71–86A
177–186A
178–187B
183–190AB
132–146A
178–187K
132–146B
133–147K
OspCK
C6–17
OspCA
OspCB

# Figure 6

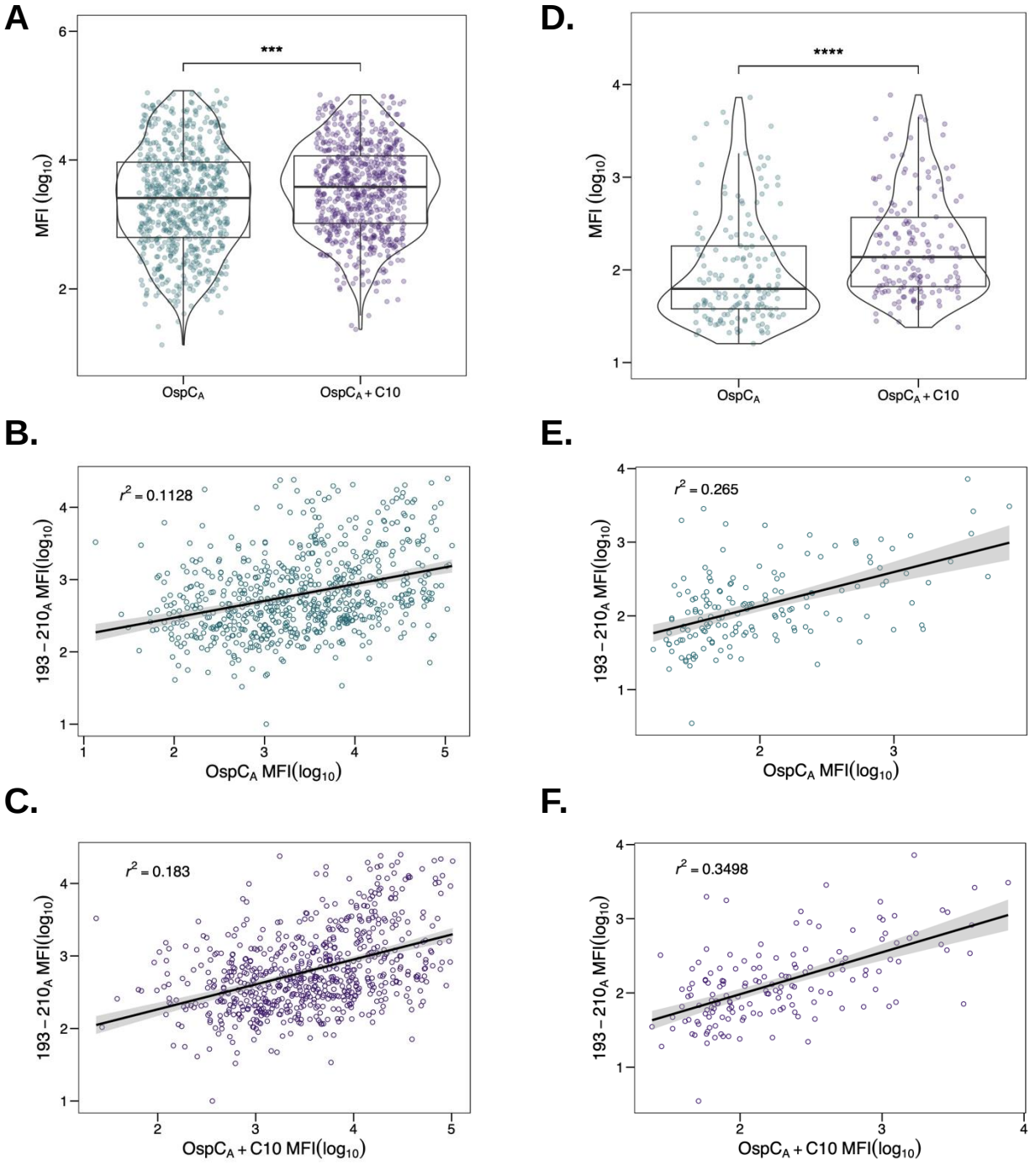
A
***
MFI (log10)
OspCA
OspCA + C10
D.
****
MFI (log10)
OspCA
OspCA + C10
B.
r2 = 0.1128
193 – 210A MFI(log10)
OspCA MFI(log10)
E.
r2 = 0.265
193 – 210A MFI(log10)
OspCA MFI(log10)
C.
r2 = 0.183
193 – 210A MFI(log10)
OspCA + C10 MFI(log10)
F.
r2 = 0.3498
193 – 210A MFI(log10)
OspCA + C10 MFI(log10)